Inorganic Chemistry

ARTICLE

pubs.acs.org/IC

Family of Cofacial Bimetallic Complexes of a Hexaanionic Carboxamide Cryptand

Glen E. Alliger, Peter Müller, Loi H. Do, Christopher C. Cummins,* and Daniel G. Nocera*

Department of Chemistry, Massachusetts Institute of Technology, 77 Massachusetts Avenue, Cambridge, Massachusetts 02139-4307, United States

Supporting Information

ABSTRACT: A series of coordination compounds has been prepared comprising manganese, iron, nickel, and zinc bound by a hexaanionic cryptand where carboxamides are anionic N-donors. The metal complexes have been investigated by X-ray crystallography, and possess metal centers in trigonal monopyramidal geometries with intermetallic distances spanning $d_{Mn,avg}$ = 6.080 Å to $d_{Ni,avg}$ = 6.495 Å. All complexes featuring trigonal monopyramidal metal(II) ions crystallize in *Cc*, and feature extended three-dimensional networks composed of cryptate anions linked by bridging potassium countercations. We also report the first solid state structure of the free cryptand ligand, which features no guest in its cavity and which possesses an extended hydrogen-bonding network. SQuID magnetometry data of the metal complexes reveal weak antiferromagnetic coupling of the metal centers. Only the diiron(II) complex exhibits reversible electrochemistry, and correspondingly, its chemical oxidation yields a powder formulated as the diiron(III) congener. The insertion of cyanide into the intermetallic cleft of the diiron(II) complex has been achieved, and comparisons of its solid state structure to the recently reported dicobalt(II) analogue are made. The antiferromagnetic coupling between the diiron(II) and the dicobalt(II) centers when bridged by cyanide does not increase significantly relative to the unbridged congeners. A one-site model satisfactorily fits Mössbauer spectra of unbridged diiron(II) and diiron(III) complexes whereas a two site fit was needed to model the iron(II) centers that are bridged by cyanide.

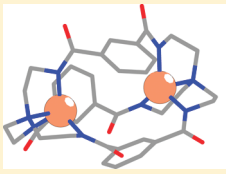

M	*M*–*M* (Å)
Mn	6.080
Fe	6.298
Co	6.408
Ni	6.495
Zn	6.423

INTRODUCTION

Designed to be three-dimensional complements to crown ethers, cryptands are unique macrocycles. Since Lehn's seminal work with polyethereal aza-cryptands,[1] the host–guest chemistry of cryptands has burgeoned, and now is prominent in the chemistry of complex cation binding,[2,3] siderophore modeling,[4,5] and electride synthesis.[6] Cryptands are particularly prominent as cation-specific sequestration reagents with binding affinities that are several orders of magnitude greater than monomacrocyclic crown ethers.[7] Size recognition properties of the cavities of smaller cryptands engender the selective sequestration of alkali and alkaline earth cations;[8] the stability constant of the potassium complex of the exemplar crypt[2.2.2] is more than an order of magnitude greater than complexes of this crypt with other alkali cations. Such selectivity finds its genesis in smaller energies of complexation for selected metal ions of incompatible size.[9] Protonated aza-cryptands have also seen use in anion sequestration.[10−12]

The advent of hexaimino-cryptands considerably expanded the cryptand class of macrocycles from monometallic binding constructs for alkali and alkaline earth cations to bimetallic binding constructs for transition metal cations.[13] Such ligands are notable not only for their binucleating ability but also for their ease of synthesis. In many cases, the condensation of 3 equiv of an aromatic dialdehyde with 2 equiv of TREN (TREN = tris(2-aminoethyl)-amine) furnishes the desired hexaiminocryptand in good yields without the need for high-dilution reaction conditions. The hydrolytic sensitivity of these ligands[14] makes their more stable octaaza counterparts, obtained from the borohydride reduction of the hexaimino-cryptand, even more attractive as ligands for binuclear complexation. To date, however, such complexes have been based on the use of ligands featuring solely charge neutral N-donors, despite the well-documented ability of triply anionic TREN moieties to complex a wide range of transition metals.[15−19]

A factor accounting for the dearth of anionic octaaza-cryptand complexes is the oxidative instability of secondary amines.[20] Incorporation of carboxamide functionalities into the ligand provides a potential means to circumvent this instability. When used as anionic N-donors, carboxamide residues are known to improve substantially the oxidative stability of ligands, and accordingly, they have enjoyed success in the stabilization of high-valent transition metal centers.[21,22] The implementation of neutral carboxamide cryptands has been explored for anion sequestration, and inclusion complexes of halides and polyoxoanions have been observed.[21−25] Nonetheless, complexes of deprotonated carboxamide-based cryptands are unusual.

We recently realized the first complex of a hexaanionic N-donor cryptand (**1**, Chart 1) with dicobalt(II) within the cleft, and demonstrated access to the intermetallic cleft through reaction with cyanide anion.[26] We now show that the method developed for double insertion of cobalt(II) into **1** can be generalized to other first-row transition metals (M = Mn through

Received: January 21, 2011
Published: March 29, 2011

Chart 1

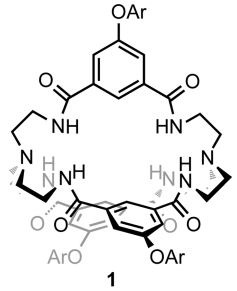

1

Ar = 3,5-dipropoxyphenyl

Zn, with the exception of Cu). The structural features and spectroscopy of these complexes presage this bitopic cryptand as a new motif to support bimetallic cooperativity.

EXPERIMENTAL SECTION

General Procedures. All manipulations were performed using either Schlenk techniques or a nitrogen-atmosphere glovebox. Reagents were purchased from Aldrich. **1** was prepared according to the previously reported synthesis by us.[26] 18-crown-6 was recrystallized from dry acetonitrile. Solvents (EMD Chemicals) were purified on a Glass Contour Solvent Purification System built by SG Water U.S.A. UV−vis spectra were obtained on a Cary 5000 spectrophotometer. IR spectra were obtained on a Perkin-Elmer Model 2000 FT-IR spectrometer. Cyclic voltammetry was performed using a BAS CV-50W Voltammetric Analyzer potentiostat. SQuID magnetometry was performed using a Quantum Design AC and DC Magnetic Property Measurement System, and data were fit using the program julX.[27] Mössbauer spectra were recorded on an MSI spectrometer (WEB Research) and referenced to metallic iron. The spectra were fit using the program WMOSS (WEB Research). Electron paramagnetic resonance (EPR) spectra were obtained on a Bruker EMX spectrometer equipped with an ER 4199HS cavity and Gunn diode microwave source. Spectra were obtained using X-band radiation. NMR solvents were obtained from Cambridge Isotope Laboratories and ^{1}H and $^{13}C\{^{1}H\}$ NMR spectra were obtained on Varian 300 and 500 MHz spectrometers and were referenced to residual protio-solvent signals. Elemental analyses were performed by Midwest Microlabs.

X-ray Crystallographic Studies. Low-temperature diffraction data were collected on a three-circle diffractometer coupled to a Bruker-AXS Smart Apex CCD detector, performing ϕ-and ω-scans, with graphite-monochromated Mo Kα radiation (λ = 0.71073 Å) for the structures of **3** and **6** and Cu Kα radiation (λ = 1.54178 Å) for the structures of **1**, **2**, **5**, and **10**. The structures were solved by direct methods using SHELXS and refined against F^2 on all data by full-matrix least-squares with SHELXL-97[28] using established methods.[29] All non-hydrogen atoms were refined anisotropically. All hydrogen atoms were included into the model at geometrically calculated positions and refined using a riding model. The isotropic displacement parameters of all hydrogen atoms were fixed to 1.2 times the *U* value of the atoms they are linked to (1.5 times for methyl groups). Disorders were refined with the help of similarity restraints on 1,2- and 1,3-distances and displacement parameters as well as rigid bond restraints for anisotropic displacement parameters. With exception of the structure of the free ligand **1**, all structures contained voids filled with heavily disordered solvent molecules. The program SQUEEZE[30] as implemented in Platon[31] was used to remove the contribution of the disordered solvent to the structure factors. Detailed information about the other structures featuring **1** as a ligand can be found in the Supporting Information of previously published work.[26]

$K_2(DMF)_6Mn_2C_{72}H_{84}N_8O_{15}$ ($[K_2(DMF)_6][Mn_2L]$, 2). A slurry of **1** (234 mg, 179 μmol) and $Mn(OAc)_2$ (62 mg, 360 μmol) was stirred in 1 mL of DMF for 30 min (Slurry 1). The mixture was frozen in the glovebox cold well, as was a solution of $KN(SiMe_3)_2$ (218 mg, 1.09 mmol, Solution 2) in 1 mL of dimethylformamide (DMF). As the slurry and solution thawed, Solution 2 was added to Slurry 1, and the mixture was allowed to warm to glovebox temperature over the course of 2 h. The reaction mixture, which turned slightly yellow over the course of the reaction, was filtered to remove precipitated potassium acetate. To the filtrate was added 10 mL of ether dropwise with rapid stirring. A white powder precipitated, and it was collected by filtration. The precipitate was washed with 12 mL of 5:1 ether/DMF and dried in vacuo. The powder comprised 183 mg (94.6 μmol, 52.8%) of analytically pure product. Elemental analysis confirms the presence of 6 DMF molecules per $K_2Mn_2C_{72}H_{84}N_8O_{15}$ unit. Crystals suitable for X-ray diffraction studies were grown by vapor diffusion of ether into a concentrated DMF solution of the product. This product is NMR silent. Anal. Calcd. (found) for $C_{90}H_{126}N_{14}O_{21}K_2Mn_2$: C, 56.06 (55.51); H, 6.59 (6.55); N 10.17 (10.45).

$K_2(DMF)_6Fe_2C_{72}H_{84}N_8O_{15}$ ($K_2(DMF)_6Fe_2L$, 3). Complex **3** was synthesized in the same fashion as complex **2**, using 1.051 g (803.8 μmol) of **1**, 278 mg (1.60 mmol) of $Fe(OAc)_2$, and 978 mg (4.90 mmol) of $KN(SiMe_3)_2$. Yield: 839 mg (435 μmol, 54.1%) of a yellow powder. ^{1}H NMR (300 MHz, DMSO-d_6, δ, all signals paramagnetically broadened): 77.34 (6 H), 62.08 (6 H), 38.60 (3 H), 7.99 (6 H), 2.87 (18 H), 2.76 (18 H), 2.26 (3 H), −0.72 (12 H) −1.06 (12 H), −1.25 (18 H), −2.00 (6 H), −4.71 (6 H), −27.61 (6 H).

$K_2(DMF)_6Ni_2C_{72}H_{84}N_8O_{15}$ ($K_2(DMF)_6Ni_2L$, 5). Complex **5** was synthesized in the same fashion as complex **2**, using 440 mg (336 μmol) of **1**, 119 mg (675 μmol) of $Ni(OAc)_2$, and 409 mg (2.05 mmol) of $KN(SiMe_3)_2$. Yield: 254 mg (131 μmol, 39.0%) of an orange-pink powder.^{1}H NMR (300 MHz, DMSO-d_6, δ, all signals paramagnetically broadened): 65.90 (6 H), 48.64 (6 H), 12.30 (3 H), 8.00 (6 H), 4.03 (6 H), 3.42 (3 H), 2.84 (18 H), 2.76 (18 H), 0.83 (6 H), 0.66 (12 H), −0.24 (12 H), −0.61 (18 H), −18.10 (6 H). Anal. Calcd (found) for $C_{90}H_{126}N_{14}O_{21}K_2Ni_2$: C, 55.85 (56.47); H, 6.56 (6.60); N 10.13 (10.23).

$K_2(DMF)_6Zn_2C_{72}H_{84}N_8O_{15}$ ($K_2(DMF)_6Zn_2L$, 6). Complex **6** was synthesized in the same fashion as complex **2** using 124 mg (95.1 μmol) of **1**, 35 mg (190 μmol) of $Zn(OAc)_2$, and 169 mg (579 μmol of $KN(SiMe_3)_2$. Yield: 98 mg (50 μmol, 53%) of a white powder.^{1}H NMR (300 MHz, DMF-d_7, δ): 7.90 (t, 3H), 6.63 (d, 6H), 6.49 (d, 6H), 6.17 (t, 3H), 4.00, (t, 12H), 3.90 (m, 6H), 2.95 (m, 6H), 2.73 (m, 6H), 2.56 (m, 6H), 1.72 (m, 12H), 0.98 (t, 18H).$^{13}C\{^{1}H\}$ NMR (75 MHz, DMSO-d_6, δ): 173.33, 162.34, 160.37, 160.29, 155.60, 143.93, 121.88, 116.20, 99.29, 96.64, 69.14, 54.16, 41.78, 35.80, 30.77, 22.08, 10.42. Anal. Calcd. (found) for $C_{90}H_{126}N_{14}O_{21}K_2Zn_2$: C, 55.46 (55.97); H, 6.52 (6.37); N 10.06 (9.26).

$[K(C_{12}H_{24}O_6)]_2Fe_2C_{72}H_{84}N_8O_{15}$ ($[K(18\text{-crown-}6)]_2$-Fe_2L, 7). A 1 mL methylene chloride solution of 22 mg (0.083 mmol, 2.9 equiv) of 18-crown-6 was added to solid stirring 56 mg (0.029 mmol, 1.0 equiv) **3**. This reaction mixture was allowed to stir for 1 h. To the solution was added 2 mL of ether, and the reaction mixture was filtered and stored in a −35 °C freezer. After several weeks, large pale yellow blocks formed. Yield: 48 mg (0.024 mmol, 82%). ^{1}H NMR (300 MHz, DMSO-d_6, δ, all signals paramagnetically broadened): 77.34 (6 H), 62.08 (6 H), 38.60 (3 H), 3.38 (48 H), 2.26 (3 H), −0.72 (12 H) −1.06 (12 H), −1.25 (18 H), −2.00 (6 H), −4.71 (6 H), −27.61 (6 H). Anal. Calcd. (found) for $C_{96}H_{132}N_8O_{27}K_2Fe_2$: C, 57.08 (57.03); H, 6.59 (6.66); N, 5.55 (5.52).

$Fe_2C_{72}H_{84}N_8O_{15}$ (Fe_2L, 8). In a 20 mL scintillation vial, 41 mg (0.16 mmol, 2.1 equiv) of silver triflate was dissolved in 2 mL of tetrahydrofuran (THF). This solution was frozen. Upon thawing, 144

dx.doi.org/10.1021/ic200143b |*Inorg. Chem.* 2011, 50, 4107–4115

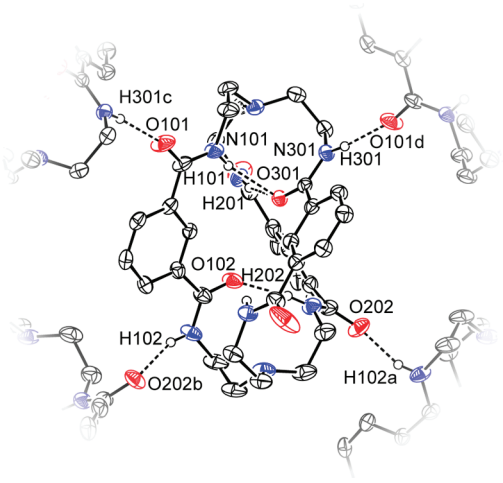

Figure 1. Solid state structure of **1**. Thermal ellipsoids at 50% probability level. Non-hydrogen bonding H atoms and dipropoxyphenoxyl substituents omitted for clarity. This view of the ligand shows both the intramolecular and intermolecular hydrogen bonding observed in the solid state.

mg (0.0746 mmol, 1.00 equiv) of **3** that was chilled to 77 K was added to the solution as a solid, and the remnants of the solid were washed in with 2 mL of THF. The reaction mixture was allowed to stir for 1.5 h, during which time it turned deep red. The reaction mixture was filtered through Celite and the filter cake was washed with THF until the washings were colorless. The filtrate was taken to dryness in vacuo, and triturated twice with hexane. The brown solid was then dissolved in 2 mL of methylene chloride, and this solution was filtered through Celite. The filtrate was taken to dryness in vacuo, and the solid so obtained was triturated twice with 2 mL of hexane. The brown solid was again dissolved in 1 mL of methylene chloride, and the solution was filtered through Celite. This was the first filtration for which no solids were observed to be removed from solution. A brown solid was precipitated from the filtrate with hexane, and it was collected. This material was subjected to Mössbauer analysis, but did not pass elemental analysis. A $CDCl_3$ solution of this solid was NMR silent.

Reduction of Fe_2L (8) with Cobaltocene. In 0.5 mL of DMSO-d_6 was dissolved 22 mg of **8**. This solution was added to a slurry of 6 mg of cobaltocene stirring in 0.5 mL of DMSO-d_6. The reaction mixture was allowed to stir for 30 min, during which time it became homogeneous. The presence of **3** was confirmed spectroscopically by ^{1}H NMR.

$[K(C_{12}H_{24}O_6)]_3Fe_2(\mu\text{-}CN)C_{72}H_{84}N_8O_{15}$ ($[K(18\text{-crown-6})]_3Fe_2(\mu\text{-}CN)L$, 10). In 3 mL of DMF was dissolved 187 mg (92.6 μmol) of $[K(18\text{-crown-6})]_2Fe_2L$ and 50 mg (190 μmol) of 18-crown-6. To this mixture was added 20 mg (0.30 mmol) of potassium cyanide. This reaction mixture was sealed in a glass thick-walled vessel and heated at 75 °C with stirring for 48 h. At this point, the reaction mixture was filtered, and the filtrate was taken to dryness. The solid product so obtained was crystallized by vapor diffusion of ether into a concentrated THF solution overnight. The resulting crystalline material was washed with 5 mL of 2:1 ether/THF and dried in vacuo. The product comprised 151 mg (64.1 μmol, 69.2%) of bright yellow crystals. Crystals suitable for X-ray analysis were grown by layering a THF solution with pentane. ^{1}H NMR (300 MHz, $CDCl_3$, δ, all signals paramagnetically broadened): 34.55 (3 H), 28.74 (3 H), 17.55 (3 H), 9.12 (3 H), 4.66 (3 H), 2.38 (12 H), 2.23 (72 H), 0.91, (12 H), 0.41 (18 H), −34.86 (3 H), −44.36 (3H), −56.13 (3 H), −71.55 (3 H). IR (Nujol, cm^{-1}): 2109 (CN). Anal. Calcd. (found) for $C_{109}H_{156}N_9O_{33}K_3Fe_2$: C, 55.72 (55.45); H, 6.69 (6.58); N, 5.37 (5.38).

Scheme 1

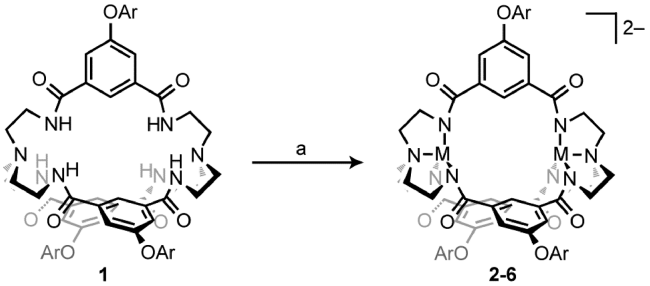

a) 2 $M(OAc)_2$, 6.1 $KN(SiMe_3)_2$, DMF, 2 h, –61 °C to 20 °C, –4 KOAc (M = Mn (**2**); Fe (**3**); Co (**4**); Ni (**5**); Zn (**6**)

RESULTS AND DISCUSSION

Synthesis. A multistep synthesis of a hexacarboxamide cryptand featuring pendant polyether moieties (**1**, Chart 1) was recently reported by us.[26] X-ray quality crystals of the cryptand **1** can be grown by vapor diffusion of ether into a THF solution. The solid-state structure is displayed in Figure 1. Coordinates for the carboxamide hydrogen atoms were taken from the difference Fourier synthesis, and the hydrogen atoms were subsequently refined semifreely, restraining the N−H distances to 0.88 Å, while constraining their U_{iso} values to 1.2 times the U_{eq} of the respective nitrogen atoms. This structure illustrates a rare example of a hexacarboxamide-cryptand that does not possess a guest molecule inside the cryptand cavity. Most "guestless" hexacarboxamide cryptands have their hydrogen bonding networks interrupted by the presence of water molecules in the crystal; a search of the Cambridge Structural Database[32,33] reveals only two such structures where this is not the case.[34,35] In contrast to metal complexes of **1**, which possess an approximate C_3 axis of symmetry (vide infra), the free ligand folds upon itself to engage in intramolecular hydrogen bonding. These hydrogen bonds from H101 and H201 to O301 (2.262(19) Å and 2.125(19) Å, respectively) and from H202 to O102 (1.925(19) Å) break the C_3 symmetry in the solid state, though this symmetry is restored on the NMR time scale for the compound in solution at room temperature. A complex variable temperature ^{1}H NMR spectrum indicates that the high symmetry is lost as a solvated sample of the cryptand is cooled to −85 °C.

The cryptand forms an extended network owing to intermolecular hydrogen bonding. Each cryptand unit in the crystal engages in four hydrogen bonds: two originate from H102 and H301, which bind to O202 and O101, respectively, in two neighboring cryptand molecules. Likewise, carboxamide oxygen atoms O201 and O102 act as receptors for hydrogen bonds from other cryptand units. H102 and H301 are 2.00(2) Å and 1.982(19) Å from their nearest acceptors, respectively. The extended network arising from intermolecular hydrogen bonding gives rise to infinite two-dimensional sheets of cryptands, with the crystallographic *c* axis oriented normal to the extended planes.

Metalation of H_6L **1** proceeds by treatment of a DMF slurry of **1** and a divalent metal acetate with a slight excess of potassium hexamethyldisilazide at low temperatures followed by warming the mixture to 25 °C over 2 h (Scheme 1). This procedure is a modification of a reported metalation protocol,[36−38] wherein metalation proceeds by deprotonation of the ligand in the presence of the metal source. This allows for introduction of

dx.doi.org/10.1021/ic200143b |*Inorg. Chem.* 2011, 50, 4107–4115

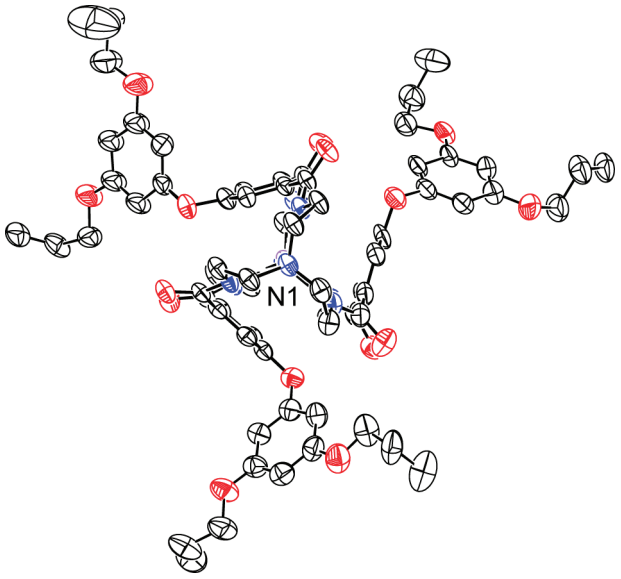

Figure 2. View of one of the cryptate units in the asymmetric unit of **2**, looking down the $N_{ap}-N_{ap}$ vector. Thermal ellipsoids at 50% probability level. H atoms, K^+ counterions, and solvents of crystallization omitted for clarity. Color scheme: black, carbon; blue, nitrogen; red, oxygen.

the metal to the ligand without the need to form a discrete hexaanionic species. After removal of precipitated potassium acetate by filtration, analytically pure material of the formula $[K_2(DMF)_6][M_2L]$ (**2**–**6**) is precipitated from the DMF solution by addition of ether. NMR spectroscopy confirms the consumption of starting material, as does the lack of a stretch representing an N–H oscillator in the infrared spectra of these materials.

Dizinc complex **6** shows a complex pattern in its ^{1}H NMR spectrum for the protons featured on the TREN methylene residues. The complex appears to be helical and rigid enough that each of the two methylene residues on any given ethylene arm of the TREN moiety are rendered diastereotopic on the NMR time scale.[39] Variable temperature NMR confirms that this behavior is maintained until at least 150 °C, though the peaks do begin to broaden at elevated temperature. Although complex **2** is NMR silent, paramagnetic species **3**–**5** exhibit well-behaved NMR spectra, with the broadening and shifting of resonances that is typical of paramagnetic compounds.[40] Protons located distal with respect to the metal centers, such as those featured on the dipropoxyphenoxyl substituents, resonate closer to the typical "diamagnetic region" of 0–10 ppm, while protons proximate to the metal center including those from the arms of the TREN moiety exhibit dramatically shifted signals. Compounds **3** and **5** display 10 paramagnetically shifted and broadened resonances (discounting those arising from DMF) in their ^{1}H NMR spectra; 9 signals should be observed based on a hypothetical D_{3h} symmetry for protons on a given TREN methylene unit equivalent. The fact that only 10 resonances are observed instead of the 11 predicted for a C_{3h}-symmetric compound is probably due to either a broadening of one resonance into the baseline or the overlap of one peak with another. The ^{1}H NMR spectrum of **4** does in fact display the expected 11 resonances.

Crystals of complexes **2**–**6** suitable for X-ray diffraction studies were grown by vapor diffusion of ether into DMF solutions of the complexes. Crystallographic studies show that compounds **2**–**6** are isostructural; they all crystallize in the same space group, *Cc*, and utilization of the same crystallographic model for all structures yields satisfactory results. In all cases, the values of R_1 are best when the identity of the metal is the same as the metal used in the synthesis. In Figure 2, the view of the anion of **2** looking down the $N_{ap}-N_{ap}$ axis reveals the dipropoxyphenoxyl substituents to be splayed out to the periphery of the cryptate. Substantial disorder is observed in the polyether component of this structure, as in the structures of **1** and other metalated cryptates. Nonetheless, the cores, defined by the TREN motifs and the phenylene spacers that span them, are ordered as shown by the representations of the anions in Figure 3.

No electron density was observed in the difference map in the void between the metal centers, ruling out the presence of apical ligands occupying the fifth coordination site of either metal center. Thus, the two metal centers are coordinated in the rare trigonal monopyramidal geometry.[15,41–50] Omission of the solubilizing substituents, potassium counterions, and solvent molecules of crystallization in Figure 3 allows for easy viewing of the intermetallic space. The metal centers are disposed in a cofacial orientation, such that the vacant coordination sites are directed toward one another. The intermetallic distance varies depending on the identity of the metal complexed, covering a range of 0.415 Å.

Figure 4 presents an overlay line drawing of the cores of complexes **2** and **6** that highlights the similarities and differences between these complexes. The metal–metal distance in **2** is the shortest of the complexes at d_{avg} = 6.080 Å. The line drawing shows that this is a result of the manganese centers puckering out of the planes defined by their respective equatorial nitrogen donors slightly. This is in contrast to **6**, which has a metal–metal distance of d_{avg} = 6.495 Å. Here, the metal center is relaxed into its TREN binding pocket. This difference of the metal residency may be due to the better size match of Zn^{2+} ion for the TREN pocket as opposed to a poorer match for the larger Mn^{2+} ion (ionic radius 0.80 Å for Mn^{2+} vs 0.74 Å for Zn^{2+}).[51] The intermetallic distance tracks with the ionic radius of the complexed metal ion (see Supporting Information). Table 1 compares and contrasts some important metrical parameters for the bimetallic crypts.

The extended structure of compounds **2**, **3**, **5**, and **6** is complex. As recently reported for isomorphous compound **4**,[26] infinite one-dimensional chains are formed by anionic cryptate units bridged by potassium cations. These one-dimensional chains are further bridged to another set of one-dimensional chains. An infinite three-dimensional extended network results from the crossing of the one-dimensional chains. This extended network may be responsible for the poor solubility properties of these materials. Compounds **2**–**6** are only soluble in highly polar organic solvents, such as DMF and dimethylsulfoxide (DMSO). Solubility in less polar solvents such as THF and methylene chloride may be imparted by introduction of 2 equiv of 18-crown-6 as previously reported for $[K(18\text{-crown-}6)]_2Co_2L$.[26] Analogous compounds, such as $[K(18\text{-crown-}6)]_2Fe_2L$ (**7**), can be crystallized by cooling a methylene chloride/ether solution of the compound.

The cyclic voltammogram of **3** (vide infra) suggests that the +3 oxidation state of iron is accessible via chemical oxidation. This indeed is the case. Treatment of **3** in DMF with silver triflate led to a darkening of the reaction mixture from golden brown to

dx.doi.org/10.1021/ic200143b |*Inorg. Chem.* 2011, 50, 4107–4115

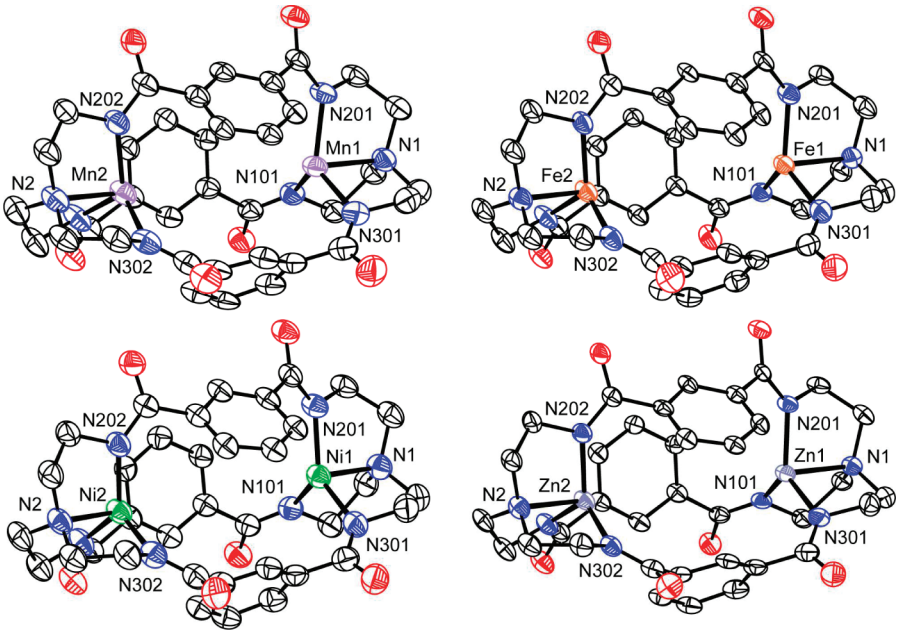

Figure 3. Solid state structure of the cores of compounds **2**, **3**, **5**, and **6**. Thermal ellipsoids at 50% probability level. H atoms, K^+ counterions, dipropoxyphenoxyl substituents, and solvents of crystallization omitted for clarity. The atom label for N102 has been omitted in all cases. See Table 1 for notable metrical parameters.

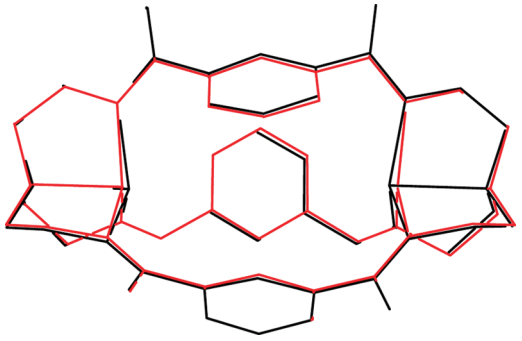

Figure 4. Overlay line drawing of **2** (black) and **6** (red).

Table 1. Comparison of Metrical Parameters for Bimetallic Cryptates[a]

metal	M−M (Å)	M−N_{ap} (Å)	Σ(N_{eq}−M−N_{eq}) (deg)	N_{ap}−N_{ap} (Å)	distance to eq. plane (Å)
Mn (**2**)	6.080	2.246	353.20	10.567	0.315
Fe (**3**)	6.298	2.180	356.17	10.654	0.229
Co (**4**)[b]	6.408	2.142	357.35	10.689	0.187
Ni (**5**)	6.495	2.064	358.73	10.616	0.128
Zn (**6**)	6.423	2.162	358.12	10.745	0.157

[a] All measurements are averages over the two cryptate units in the asymmetric unit. [b] From ref 26.

deep crimson. Removal of the solvent and subsequent workup led to the isolation of a brown powder that we have formulated as the impure diiron(III) cryptate, **8**. This species would be expected to have no extended network of anions bridged by potassium counter-cations, and it is freely soluble in solvents such as THF and methylene chloride. This complex does not pass elemental analysis, and attempts to crystallize it have not yet met with success. While it is not clear what has prevented the isolation of this compound in pure form, it should be noted that difficulty in the characterization of oxidation products of trigonal monopyramidal iron(II) has been observed previously.[43] Analysis of the worked-up material by Mössbauer spectroscopy (vide infra) suggests the presence of one high spin iron(III) environment. Treatment of this as-isolated material with two equiv of cobaltocene results in reduction of **8** to the dicobaltocenium analogue of **3**, as judged by ^{1}H NMR spectroscopy, wherein the potassium counter-cations have been replaced with cobaltocenium cations without any loss of solubility.

Cyanide ion may be included between the metals of the cryptand cavity. As reported for the conversion of **4** to [K(18-crown-6)]$_3$Co$_2$(μ-CN)L (**9**), cyanide ion can be inserted into the intermetallic region of **3** to give the bridging cyanide complex, [K(18-crown-6)]$_3$Fe$_2$(μ-CN)L, **10**. As with **9**, compound **10** displays more resonances in its ^{1}H NMR spectrum than that of its unbridged analogue **3**; this is in keeping with the breaking of mirror plane symmetry upon addition of cyanide. A single crystal of **10** grown from a THF solution layered with pentane was subjected to X-ray analysis, and the solid-state structure shown in Figure 5 was deduced. Crystals of **10** are isomorphous with crystals of **9**, crystallizing in $P\bar{1}$ and having unit cells that differ by only 9 Å^3. The cyano ligand is also disordered end over end; the ratio of cryptate units possessing a cyano ligand that is C-bound to Fe1 versus N-bound is 52%, which is comparable to the value found for the cobalt congener (63%). Complex **10** displays a longer M2−C3 bond than **9** (2.13(2) Å in **10** vs 2.074(18) Å in **9**), and similar M1−N3 (2.12(2) Å in **10** vs 2.100(14) Å in **9**) and C3−N3 bond distances (1.149(12) Å in **10** vs 1.159(1) Å in **9**). A C−N stretch appears at 2109 cm^{-1} in the infrared spectrum of **10** as compared to 2129 cm^{-1} for **9**. Although the C3−N3 distances in **9** and **10** are essentially unchanged relative to the C−N distance of 1.16 Å in free cyanide,[52] the observed infrared stretches are higher in energy than that of free cyanide anion (2080 cm^{-1}).[53] This observation suggests minimal

dx.doi.org/10.1021/ic200143b |*Inorg. Chem.* 2011, 50, 4107–4115

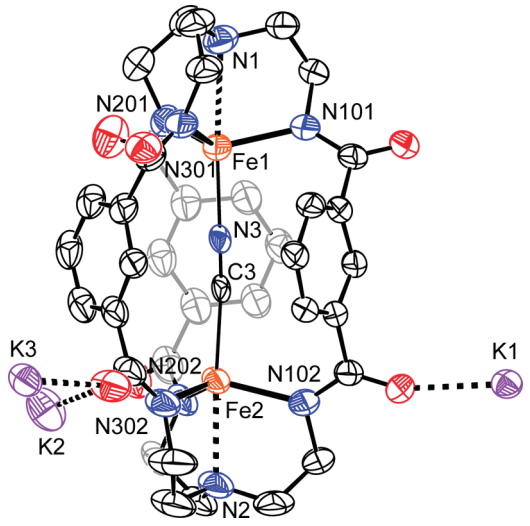

Figure 5. Solid state structure of the core of compound **10**. Thermal ellipsoids at 50% probability level. H atoms, dipropoxyphenoxyl substituents, crown ethers, and solvents of crystallization omitted for clarity. One phenylene spacer has been grayed for ease of viewing. Notable metrics: Fe1−N3: 2.12(2) Å, Fe2−C3: 2.13(2) Å, C3−N3: 1.149(12) Å, Fe1−Fe2: 5.3869(1) Å, $\Sigma(N_{eq}-Fe1-N_{eq})$ = 340.83(26)°; $\Sigma(N_{eq}-Fe2-N_{eq})$ = 344.10(29)°.

backbonding between the metals and the bridging cyanide. The depletion of electron density from the CN^- σ^* orbital is likely responsible for the observed increase in the CN frequency of **9** and **10**.[54]

Mössbauer Studies. Low-temperature Mössbauer spectra of iron complexes **3**, **8**, and **10** are presented in Figure 6. The Mössbauer spectrum of **3** was obtained at 80 K, and this spectrum was fit by simulation using a single site, in accordance with the symmetry of the complex. The spectrum consists of a single quadrupole doublet centered at δ = 0.80 mm/s, with a quadrupole splitting of ΔE_Q = 1.09 mm/s. These values fall in the standard range for high spin iron(II) complexes,[39] though they are notably different than the values for the trigonal monopyramidal iron(II) complex $[\{N(CH_2CON^tPr)_3\}Fe]^-$ (δ = 1.05 mm/s and ΔE_Q = 3.31 mm/s).[42] The main features in the spectrum of **3**, as well as spectra obtained for the other iron complexes discussed here, are quite broad (line width = ca. 0.7 mm/s) when obtained at liquid nitrogen temperatures. The origin of the observed broadening is not immediately clear, and there is little information on the Mössbauer spectra of trigonal monopyramidal iron(II) to serve as a guide for what to expect. One potentially germane benchmark is trigonal monopyramidal mononuclear iron(II) species of the tris(phenylamido)amine scaffold.[50] In the Mössbauer spectrum of this compound, two species are observed, both of which appear to be high spin iron(II) (δ = 0.75 mm/s and ΔE_Q = 0.91 mm/s (Site 1) and δ = 0.76 mm/s and ΔE_Q = 1.43 mm/s (Site 2)). Minor asymmetries in the ligand field about the metal centers, as the compound crystallizes as a potassium-bridged dimer, are invoked to explain the presence of two sites in the Mössbauer spectrum. Given that **3** displays a broad spectrum at low *T*, and possesses four iron(II) sites (two cryptate units per unit cell) that are slightly inequivalent in the solid state, we considered the possibility of a multiple site fit for the Mössbauer data for this compound. However, a simple one site fit does, in fact, yield a satisfactory

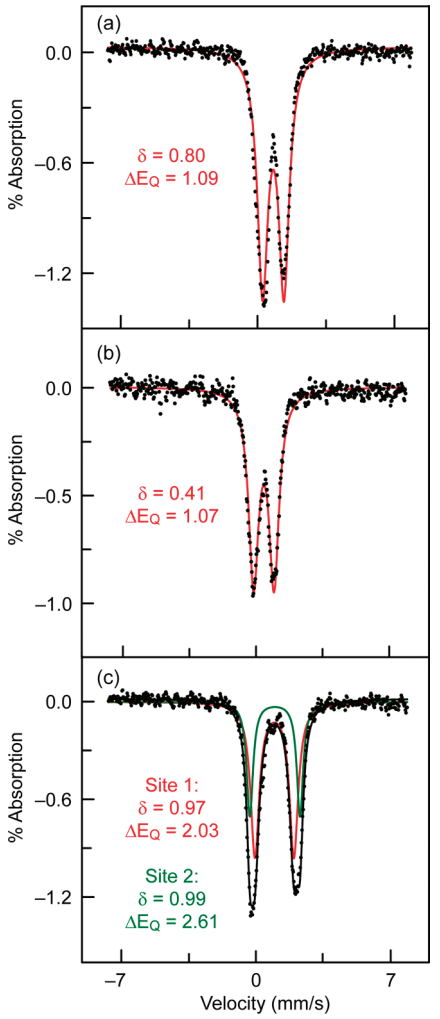

Figure 6. Mössbauer spectra of (a) **3**, (b) **8**, and (c) **10**. Samples collected on polycrystalline samples at 80 K (**3** and **8**) or 5 K (**10**).

model, excepting the unusually large linewidths. The spectrum does sharpen considerably upon acquisition at higher temperatures (250 K), with line widths dropping to about 0.45 mm/s; these data are also satisfactorily fit with a one site model.

The Mössbauer spectrum of **8** (Figure 6b) at 80 K displays a single quadrupole doublet with an isomer shift of 0.41 mm/s, and a quadrupolar splitting of 1.07 mm/s, indicating that the sample is pure in iron, though it does not pass elemental analysis. While the linewidths are again quite broad (line width = ca. 0.8 mm/s), the parameters obtained by a single-site fit suggest that the complex indeed contains high-spin iron(III). At 5 K, this compound exhibits a complex spectrum that is difficult to interpret but is characteristic of a magnetic sample with slow electronic relaxation.[39] Again, Mössbauer spectra of trigonal monopyramidal iron(III) have not been reported, but the spectra of related compounds, $[N\{CH_2CH_2NCO\text{-}NH^tBu\}_3FeO]^{2-}$ and $[N\{CH_2CH_2NC(O)NH^tBu\}_3FeOH]^-$, also display complex spectra at liquid helium temperature, presumably because of slow electronic relaxation. At 77 K, the signals collapse to quadrupole doublets with δ = 0.30 mm/s, ΔE_Q = 0.71 mm/s and δ = 0.32 mm/s, ΔE_Q = 0.92 mm/s, respectively.[55] Another related trigonal iron(III) compound, $Fe[N(SiMe_3)_2]_3$,[56] which has been structurally characterized,[57] displays parameters of δ =

dx.doi.org/10.1021/ic200143b |*Inorg. Chem.* 2011, 50, 4107–4115

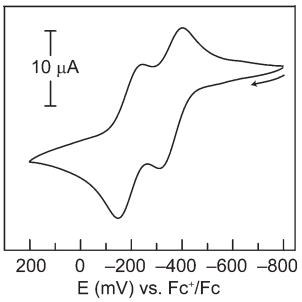

Figure 7. Cyclic voltammogram of compound **3**, referenced to ferrocenium/ferrocene.

0.30 mm/s and ΔE_Q = 5.12 mm/s.[58,59] Of note is the fact that the spectrum of this compound is broadened significantly because of slow electronic relaxation, though in contrast to the low temperature spectrum of **8**, only one peak of the quadrupole doublet experiences this effect.

The spectrum of the bridging cyanide complex **10**, shown in Figure 6c, is best modeled by a superposition of two signals, indicating that **10** possesses two inequivalent sites. The two signals overlap and display very similar isomer shifts: the parameters for the two sites are δ = 0.97 mm/s, ΔE_Q = 2.03 mm/s and δ = 0.99 mm/s, ΔE_Q = 2.61 mm/s. The similarity of the isomer shifts can be ascribed to the qualitative similarity of the iron environments. Both are tetrahedral iron(II), differing only in the atom, C or N, of the cyanide ligand that coordinates to the metal center. Because the magnitude of the quadrupole splitting decreases with increasing covalency of a given iron center's coordination sphere, we assign the signal of smaller quadrupole splitting at δ = 0.97 mm/s to the iron center that is C-bound to the cyanide ligand.[60] As such, the signal with the larger quadrupole splitting at δ = 0.99 mm/s is assigned to the iron that is N-bound to the cyanide.

Electrochemistry. Whereas complexes **2**, **4**, and **5** display irreversible oxidations at potentials positive of ferrocene (see Supporting Information, Figure S1), **3** displays reversible electrochemical behavior. The cyclic voltammogram in Figure 7 exhibits two reversible one electron waves at −148 mV and −309 mV relative to ferrocene. The difference between the two oxidation potentials, ΔE_{ox}, is equal to 161 mV, which equates to a comproportionation constant[61] of 536. The separation of the electrochemical waves suggests that a mixed valent Fe(II)/Fe(III) species may be accessible.

The electrochemistry of **10** (Supporting Information, Figure S1) shows that the reversible electrochemistry observed for **3** is lost upon insertion of the bridging cyanide. An irreversible reduction event is observed at −3 V vs Fc/Fc$^+$, which feature remains irreversible with increasing scan rate. Scanning anodically, irreversible oxidation events are observed at −970 and 620 mV vs Fc/Fc$^+$. These events also remain irreversible with increasing scan rate. Scanning anodically before scanning cathodically reveals that the oxidation peaks are not observed until the potential is swept through the reduction event.

EPR Studies. Figure 8 presents the low temperature (4.2 K) X-band EPR spectra for complexes **2** and **4** as frozen DMF solutions. The broad features in these spectra are not believed to be due to aggregation, as less concentrated samples do not display sharper spectra. The cobalt species displays an axial spectrum with $g_{||}$ = 4.61 and $g_\perp$ = 1.70, and no hyperfine coupling

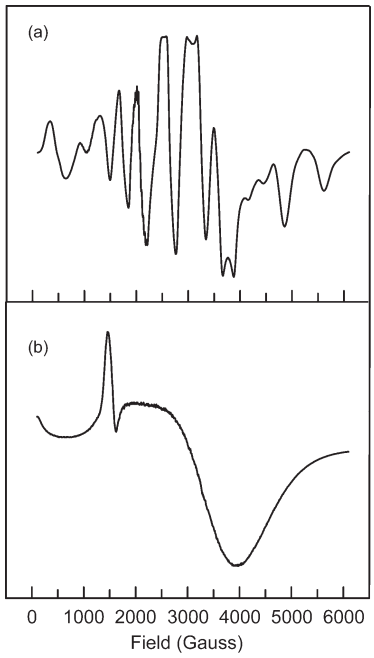

Figure 8. EPR spectra at 4.2 K for (a) **2** and (b) **4**. Spectra obtained as frozen DMF solutions at X-band frequency.

is observed. Manganese and cobalt complexes of trigonal monopyramidal geometry are very rare. No EPR spectra are reported for the few examples of trigonal monopyramidal manganese(II) complexes,[15] and in only one case has a trigonal monopyramidal cobalt(II) complex been characterized by EPR.[43] The signal observed in the case of this compound is broad, with a g value of 4.17.

Conversely, trigonal bipyramidal cobalt(II) complexes are more common, and they exhibit EPR spectra that qualitatively resemble that of **4**. The X-band EPR spectrum of pentakis(picoline-*N*-oxide)cobalt(II) perchlorate displays a broad spectrum having g_1 = 5.67, g_2 = 3.53 and g_3 = 1.86.[62] In this case, g_1 and g_3 match the spectrum of **4** fairly well, though the spectrum of **4** lacks an analogous g_2 feature. The EPR spectrum of [CoBr(Me$_6$TREN)]Br qualitatively matches that of **4** nicely, and has parameters of $g_{||}$ = 2.27 and $g_\perp$ = 4.30.[63] Note that the assignment of $g_{||}$ and $g_\perp$ are opposite to those assigned in **4**. This is due to the fact that for [CoBr(Me$_6$TREN)]Br, the magnitude of the feature at g = 2.27 is larger than that at g = 4.30. This is the reverse of what is observed for **4**; further experiments would be required to definitively assign the identities of the g-values. The EPR spectra of trigonal bipyramidal manganese(II) complexes contain, in general, features that are broad and difficult to interpret. For example, [Mn$_2$(TREN)$_2$(NCO)$_2$](BPh$_4$)$_2$ displays a very broad signal covering a large magnetic field range, with several features that could not be confidently assigned.[64] Even the EPR spectrum of manganese in pseudotetrahedral fields is difficult to interpret and simulate.[65]

Magnetism. SQuID magnetometric data for the unbridged bimetallic cryptates is provided in Figure 9. In each case, a fit of the magnetic data to the Hamiltonian,

$$\hat{H} = -J\hat{S}_A \cdot \hat{S}_B + \hat{S}_A \cdot D_A \cdot \hat{S}_A + \hat{S}_B \cdot D_B \cdot \hat{S}_B + \beta(\hat{S}_A \cdot g_A + \hat{S}_B \cdot g_B) \cdot B$$

using the program julX,[27] supports the formulation of the complexes as high-spin at high temperature. The first term

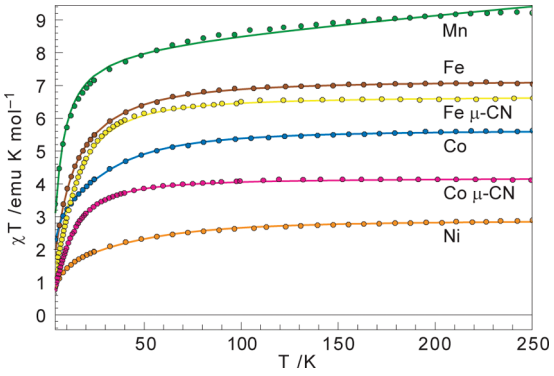

Figure 9. SQuID data for bimetallic cryptates **2**, **3**, **4**, **5**, **9**, and **10**.

Table 2. Magnetic Parameters for Bimetallic Cryptates

compound	J_{12} (cm^{-1})	g	$\mu_{eff}{}^{a}$	$\mu_{eff}{}^{b}$
Mn (**2**)	−0.1	2.0	8.57	8.37
Fe (**3**)	−0.3	2.2	7.52	6.93
Co (**4**)	−0.3	2.5	6.69	5.47
Ni (**5**)	−0.7	2.4	4.77	4.00
Co-μ-CN (**9**)	−0.7	2.1	5.76	5.47
Fe-μ-CN (**10**)	−0.4	2.1	7.26	6.93

[a] Room temperature, observed. [b] Expected spin-only value.

represents the exchange Hamiltonian, the second and third terms introduce the effect of the local anisotropy of the metal centers, and the last term represents the Zeeman splitting.[66] Because of the approximate C_{3h} symmetry of the complexes, S_A was constrained to be equal to S_B in all cases. The anisotropy tensors for both centers were also constrained to be equivalent, as were the g-tensors for all fits.

A summary of the findings gleaned from the magnetic data is compiled in Table 2. The magnetic measurements confirm formulations of the bimetallic cryptates as high spin complexes in all cases. The magnetic coupling between the metal centers is antiferromagnetic and extremely weak ($0 > J > -1$ cm^{-1}). This result is in line with expectations, given that the complexes feature through-space metal−metal distances in excess of 6 Å, an exceedingly long distance for strong coupling.[67,68] The shortest through-bond pathway in the complexes occurs over a 7-atom pathway; couplings of about 1 cm^{-1} are consistent with superexchange over 7-atom pathways.[69,70]

SQuID magnetic data for **9** and **10**, as well as the fits of the data (obtained in the same fashion as those for the unbridged species discussed above), appear in Figure 9; information obtained from these fits is presented in Table 2. The metal centers in these complexes are antiferromagnetically coupled, as they are in the parent complexes. The exchange coupling might be expected to significantly increase for two metal centers bridged by a two atom linear bridge.[54] However, this is not the case for the cyanide complexes. The peculiarly long distance between the metal centers in both **9** and **10**, most likely enforced by the phenylene spacers, may be playing a role in attenuating the coupling. The metal−metal distances in these complexes of 5.3869(10) Å and 5.3263(9) Å, respectively, are longer than any Fe−C≡N−Fe or Co−C≡N−Co distances reported in the Cambridge Structural Database.[32,33] Moreover, the observation of weak metal-cyanide π-backbonding in the infrared spectra (vide supra) points to ineffective overlap between the metal d orbitals and the orbitals of the cyanide ligand.[71]

CONCLUSIONS

The hexacarboxamide ligand and their metal complexes reported herein expand the chemistry of cryptands. The sextuply anionic cryptand can support two metals from the first row within its cleft of +2 oxidation state. The diiron(II) complex exhibits reversible electrochemistry, and we have reported here initial investigations into the isolation of the analogous diiron(III) complex; work in this area is ongoing. Complexation of cyanide anion to the iron centers in the diiron(II) complex results in a bridging cyano species, in analogy to the previously reported dicobalt(II) bridging cyanide. Magnetic analysis of these unbridged divalent metal complexes and the bridging cyanide complexes show that they are very weakly antiferromagnetically coupled. The studies reported herein establish the hexacarboxamide ligand as a general scaffold for the cofacial positioning of trigonal metal sites and opens avenues for cooperative redox and substrate binding.

ASSOCIATED CONTENT

Supporting Information. Crystallographic details and cif files, CV data for compounds **2**, **5**, and **10**, and UV/vis data for compounds **2**, **3**, and **5**. This material is available free of charge via the Internet at http://pubs.acs.org.

AUTHOR INFORMATION

Corresponding Author

*E-mail: ccummins@mit.edu (C.C.C.); nocera@mit.edu (D.G.N.).

ACKNOWLEDGMENT

The compounds were discovered under the sole sponsorship of Eni S.p.A under the Eni-MIT Alliance Solar Frontiers Program. Characterization work was performed under grants from the NSF (CHE-0533150 and CHE-0802907). The authors thank Prof. S. J. Lippard for the use of his Mössbauer spectrometer.

REFERENCES

(1) Dietrich, B.; Lehn, J. M.; Sauvage, J. P. *Tetrahedron Lett.* **1969**, *10*, 2885–2888.
(2) Chekhlov, A. N. *J. Struct. Chem.* **2003**, *44*, 335–339.
(3) Allwood, B. L.; Kohnke, F. H.; Stoddart, J. F.; Williams, D. J. *Angew. Chem., Int. Ed. Engl.* **1985**, *24*, 581–584.
(4) Cohen, S. M.; Petoud, S.; Raymond, K. N. *Inorg. Chem.* **1999**, *38*, 4522–4529.
(5) McMurry, T. J.; Hosseini, M. W.; Garrett, T. M.; Hahn, F. E.; Reyes, Z. E.; Raymond, K. N. *J. Am. Chem. Soc.* **1987**, *109*, 7196–7198.
(6) Dye, J. L. *Acc. Chem. Res.* **2009**, *42*, 1564–1572.
(7) Steed, J. W.; Atwood, J. L. *Supramolecular Chemistry*; Wiley: Chichester, 2009.
(8) Dietrich, B.; Lehn, J. M.; Sauvage, J. P.; Blanzat, J. *Tetrahedron* **1973**, *29*, 1629–1645.
(9) Kauffmann, E.; Lehn, J. M. *Helv. Chim. Acta* **1976**, *59*, 1099–1111.
(10) Kintzinger, J. P.; Lehn, J. M.; Kauffmann, E.; Dye, J. L.; Popov, A. I. *J. Am. Chem. Soc.* **1983**, *105*, 7549–7553.
(11) Nelson, J.; Nieuwenhuyzen, M.; Pal, I.; Town, R. M. *Dalton Trans.* **2004**, 229–235.

(12) Ravikumar, I.; Lakshminarayanan, P. S.; Suresh, E.; Ghosh, P. *Inorg. Chem.* **2008**, *47*, 7992–7999.
(13) MacDowell, D.; Nelson, J. *Tetrahedron Lett.* **1988**, *29*, 385–386.
(14) Harding, C. J.; Lu, Q.; Malone, J. F.; Marrs, D. J.; Martin, N.; McKee, V.; Nelson, J. *Dalton Trans.* **1995**, 1739–1747.
(15) Cummins, C. C.; Lee, J.; Schrock, R. R.; Davis, W. D. *Angew. Chem., Int. Ed. Engl.* **1992**, *31*, 1501–1503.
(16) Cummins, C. C.; Schrock, R. R. *Inorg. Chem.* **1994**, *33*, 395–396.
(17) Cummins, C. C.; Schrock, R. R.; Davis, W. M. *Organometallics* **1992**, *11*, 1452–1454.
(18) Cummins, C. C.; Schrock, R. R.; Davis, W. M. *Angew. Chem., Int. Ed. Engl.* **1993**, *32*, 756–759.
(19) Cummins, C. C.; Schrock, R. R.; Davis, W. M. *Inorg. Chem.* **1994**, *33*, 1448–1457.
(20) Keene, R. F. *Coord. Chem. Rev.* **1999**, *187*, 121–149.
(21) Chanda, A.; Popescu, D.-L.; de Oliveira, F. T.; Bominaar, E. L.; Ryabov, A. D.; Münck, E.; Collins, T. J. *J. Inorg. Biochem.* **2006**, *100*, 606–619.
(22) Miller, C. G.; Gordon-Wylie, S. W.; Horwitz, C. P.; Strazisar, S. A.; Peraino, D. K.; Clark, G. R.; Weintraub, S. T.; Collins, T. J. *J. Am. Chem. Soc.* **1998**, *120*, 11540–11541.
(23) Bowman-James, K. *Acc. Chem. Res.* **2005**, *38*, 671–678.
(24) Ghosh, S.; Roehm, B.; Begum, R. A.; Kut, J.; Hossain, M. A.; Day, V. W.; Bowman-James, K. *Inorg. Chem.* **2007**, *46*, 9519–9521.
(25) Kang, S. O.; Llinares, J. M.; Powell, D.; VanderVelde, D.; Bowman-James, K. *J. Am. Chem. Soc.* **2003**, *125*, 10152–10153.
(26) Alliger, G. E.; Müller, P.; Cummins, C. C.; Nocera, D. G. *Inorg. Chem.* **2010**, *49*, 3697–3699.
(27) julX is a freely available program created by E. Bill for the simulation and analysis of magnetic data. It may be downloaded at http://ewww.mpi-muelheim.mpg.de/bac/ logins/bill/julX_en.php.
(28) Sheldrick, G. M. *Acta Crystallogr.* **2008**, *A64*, 112–122.
(29) Müller, P. *Crystallogr. Rev.* **2009**, *15*, 57–83.
(30) van der Sluis, P.; Spek, A. L. *Acta Crystallogr.* **1990**, *A46*, 194–201.
(31) Spek, A. *Acta Crystallogr.* **2009**, *D65*, 148–155.
(32) Allen, F. H. *Acta Crystallogr.* **2002**, *B58*, 380–388.
(33) Search of Cambridge Structural Database performed on July 12, 2010.
(34) Lai, J.-L.; Leung, M.-k.; Lee, G. H. *J. Org. Chem.* **1996**, *61*, 8364–8365.
(35) Colin, J. C.; Mallah, T.; Journaux, Y.; Mollar, M.; Lloret, F.; Julve, M.; Boubekeur, K. *Inorg. Chim. Acta* **1996**, *246*, 249–258.
(36) Yandulov, D. V.; Schrock, R. R.; Rheingold, A. L.; Ceccarelli, C.; Davis, W. M. *Inorg. Chem.* **2003**, *42*, 796–813.
(37) Weare, W. W.; Schrock, R. R.; Hock, A. S.; Müller, P. *Inorg. Chem.* **2006**, *45*, 9185–9196.
(38) Wampler, K. M.; Schrock, R. R. *Inorg. Chem.* **2007**, *46*, 8463–8465.
(39) Drago, R. S. *Physical Methods for Chemists*, 2nd ed.; Surfside Scientific: Gainesville, FL, 1992.
(40) *NMR of Paramagnetic Molecules: Principles and Applications*; La Mar, G. N., Horrocks, D. W., Holm, R. H., Eds.; Academic Press: New York, 1973.
(41) Ray, M.; Yap, G. P. A.; Rheingold, A. L.; Borovik, A. S. *J. Chem. Soc., Chem. Commun.* **1995**, 1777–1778.
(42) Ray, M.; Golombek, A. P.; Hendrich, M. P.; Young, V. G.; Borovik, A. S. *J. Am. Chem. Soc.* **1996**, *118*, 6084–6085.
(43) Ray, M.; Hammes, B. S.; Yap, G. P. A.; Rheingold, A. L.; Borovik, A. S. *Inorg. Chem.* **1998**, *37*, 1527–1532.
(44) Borovik, A. S. *Acc. Chem. Res.* **2004**, *38*, 54–61.
(45) Filippou, A. C.; Schneider, S.; Schnakenburg, G. *Inorg. Chem.* **2003**, *42*, 6974–6976.
(46) Greenwood, B. P.; Rowe, G. T.; Chen, C.-H.; Foxman, B. M.; Thomas, C. M. *J. Am. Chem. Soc.* **2009**, *132*, 44–45.
(47) Schrock, R. R. *Acc. Chem. Res.* **1997**, *30*, 9–16.
(48) Das, U. K.; Bobak, J.; Fowler, C.; Hann, S. E.; Petten, C. F.; Dawe, L. N.; Decken, A.; Kerton, F. M.; Kozak, C. M. *Dalton Trans.* **2010**, *39*, 5462–5477.
(49) Jones, M. B.; MacBeth, C. E. *Inorg. Chem.* **2007**, *46*, 8117–8119.
(50) Paraskevopoulou, P.; Ai, L.; Wang, Q.; Pinnapareddy, D.; Acharyya, R.; Dinda, R.; Das, P.; Çelenligil-Çetin, R.; Floros, G.; Sanakis, Y.; Choudhury, A.; Rath, N. P.; Stavropoulos, P. *Inorg. Chem.* **2009**, *49*, 108–122.
(51) Cotton, F. A.; Wilkinson, G.; Murillo, C. A.; Bochmann, M. *Advanced Inorganic Chemistry*, 6th ed.; Wiley: New York, 1999.
(52) Elliott, N.; Hastings, J. *Acta Crystallogr.* **1961**, *14*, 1018.
(53) Nakamoto, K. *Infrared and Raman Spectra of Inorganic and Coordination Compounds, Part A: Theory and Applications in Inorganic Chemistry*; Wiley: New York, 1997.
(54) Shatruk, M.; Avendano, C.; Dunbar, K. R. In *Prog. Inorg. Chem.*; Karlin, K., Ed.; Wiley: Hoboken, NJ, 2009; Vol. 56, pp 155−334.
(55) MacBeth, C. E.; Golombek, A. P.; Young, V. G.; Yang, C.; Kuczera, K.; Hendrich, M. P.; Borovik, A. S. *Science* **2000**, *289*, 938–941.
(56) Bürger, H.; Wannagat, U. *Monatsh. Chem.* **1963**, *94*, 1007–1012.
(57) Bradley, D. C.; Hursthouse, M. B.; Rodesiler, P. F. *J. Chem. Soc. D, Chem. Commun.* **1969**, 14–15.
(58) Alyea, E. C.; Bradley, D. C.; Copperthwaite, R. G.; Sales, K. D.; Fitzsimmons, B. W.; E, J. C. *J. Chem. Soc. D, Chem. Commun.* **1970**, 1715–1716.
(59) Fitzsimmons, B. W.; Johnson, C. E. *Chem. Phys. Lett.* **1974**, *24*, 422–424.
(60) Vértes, A.; Korecz, L.; Burger, K. In *Mössbauer Spectroscopy*; Elsevier: Amsterdam, The Netherlands, 1979, p 139.
(61) Richardson, D. E.; Taube, H. *Inorg. Chem.* **1981**, *20*, 1278–1285.
(62) Bencini, A.; Benelli, C.; Gatteschi, D.; Zanchini, C. *Inorg. Chem.* **1980**, *19*, 3839–3841.
(63) Benelli, C.; Gatteschi, D. *Inorg. Chem.* **1982**, *21*, 1788–1790.
(64) Laskowski, E. J.; Hendrickson, D. N. *Inorg. Chem.* **1978**, *17*, 457–470.
(65) King, E. R.; Betley, T. A. *J. Am. Chem. Soc.* **2009**, *131*, 14374–14380.
(66) Kahn, O. *Molecular Magnetism*; VCH Publishers: New York, 1993.
(67) Verdaguer, M. *Polyhedron* **2001**, *20*, 1115–1128.
(68) Coffman, R. E.; Buettner, G. R. *J. Phys. Chem.* **1979**, *83*, 2387–2392.
(69) Itoh, K.; Minoru, K. *Molecular Magnetism*; Kodansha: Tokyo, 2000.
(70) Papoutsakis, D.; Kirby, J. P.; Jackson, J. E.; Nocera, D. G. *Chem.—Eur. J.* **1999**, *5*, 1474–1480.
(71) Beltran, L. M. C.; Long, J. R. *Acc. Chem. Res.* **2005**, *38*, 325–334.